

Micropatternable elastic electrets based on a PDMS/carbon nanotube composite

This article has been downloaded from IOPscience. Please scroll down to see the full text article.

2010 J. Micromech. Microeng. 20 104003

(<http://iopscience.iop.org/0960-1317/20/10/104003>)

View [the table of contents for this issue](#), or go to the [journal homepage](#) for more

Download details:

IP Address: 130.207.50.192

The article was downloaded on 20/01/2011 at 15:21

Please note that [terms and conditions apply](#).

Micropatternable elastic electrets based on a PDMS/carbon nanotube composite

W J Xu¹, M Kranz², S H Kim² and M G Allen²

¹ School of Polymer, Textile and Fiber Engineering, Georgia Institute of Technology, 801 Ferst Drive, MRDC 1, Atlanta, GA 30332, USA

² School of Electrical and Computer Engineering, Georgia Institute of Technology, 791 Atlantic Drive, Atlanta, GA 30332, USA

E-mail: wxu3@gatech.edu

Received 1 March 2010, in final form 25 June 2010

Published 14 September 2010

Online at stacks.iop.org/JMM/20/104003

Abstract

This paper reports the fabrication and performance of an elastic electret based on polydimethylsiloxane (PDMS)/carbon-nanotube (CNT) nanocomposites. The composite formulation concentrates CNTs near the surface of the PDMS and thereby combines the excellent electrical properties and room temperature micropatternability of the CNT with the elasticity of PDMS. The fabrication approach preserves the good rheological properties of unfilled PDMS and also efficiently utilizes the CNTs. The material was corona charged and the charge storage behavior was characterized using surface potential measurements. Substantial improvements in charge storage capacity and stability were observed compared to either pure PDMS or CNTs on the surface of PDMS at room temperature over a 280 h measurement period. The power generation of the corona-charged elastic composite was initially demonstrated through a ball drop experiment.

(Some figures in this article are in colour only in the electronic version)

1. Introduction

An electret is a dielectric which exhibits quasi-permanent electric charge or dipole moment. Electrets have been demonstrated in multiple applications such as microphones, micro power generators, piezoelectric sensors/actuators, microfluidic devices, biomedical implants and organic field effect transistor memories [1–4]. Based on different charge storage mechanisms, electrets can be approximately classified into four types, as summarized in table 1. Traditional electret materials such as the silicon dioxide/silicon nitride double layer, and thin film fluoropolymers such as Teflon AF[®] and CYTOP[®], possess the key electret properties of high surface charge density and long-term charge stability. Amjadi reported a negatively charged SiO₂/SiN_x double layer that exhibited charge retention capability of over 3 years when being properly stored in a box [5]. However, the SiO₂/SiN_x usually requires high processing temperature (>500 °C) [5] and the electret film produced from these materials is rigid with Young's modulus of over 40 GPa, which may compromise its applicability in flexible devices. Teflon has limited solubility in few selected

fluorinated solvents, which brings an issue to its processability [6]. CYTOP[®] is one of the state-of-the-art electrets which can be spin coated and have demonstrated surface charge density of 1.3 mC m⁻² and good charge storage stability for over 4000 h [7]. Yet both Teflon and CYTOP[®] have relatively high Young's moduli (0.5 GPa and 1.2 GPa, respectively) [8]. It is therefore useful to develop an electret material bearing good micropatternability, low processing temperature and mechanical flexibility/elasticity all at the same time.

Squeezable/elastic electrets may expand the utility of electrets in many applications, including skin-like energy harvesters that could be pervasively integrated into existing electronic systems simultaneously and tap environmental sources such as human or object motion to generate power. In addition, the use of an elastomer in electrets can enhance piezoelectric transduction. The piezoelectric coefficient of an electret, d_{33} , can be determined by the following equation [9]:

$$d_{33} = 2\eta\sigma_s/E_y, \quad (1)$$

where σ_s is the surface charge density and E_y is the Young modulus of the material. Therefore, a lower E_y can lead

Table 1. Types of electrets [5, 17, 18].

Electret material	Dominant charge storage mechanism	Charge density (mC m ⁻²)	Young's modulus (GPa)	Piezoelectric coefficient (pC N ⁻¹)
Non-polar polymers (Teflon, PE, PP)	Space/bulk charge	<6 (0.5 for Teflon AF [®])	1–3	0.1–1.0
Polar polymers (CYTOP [®] , Parylene)	Dipole moment	<63 (1.37, 3.69)	2–4	0.1–3.0
SiO ₂ /SiN _x	Interface charge	11.5	40–70/100–300	N/A
Porous polymer (cellular PP, PTFE)	Charges in the interface of the voids	<2.1	6 × 10 ⁻⁶ –1 × 10 ⁻³	<300

to a higher d_{33} . Most traditional inorganic or polymeric electrets have a relatively high E_y , typically in the range of 1–100 GPa, while elastomeric materials have a much lower E_y , typically several MPa. As illustrated in table 1, cellular polymeric electrets with a low E_y exhibit much higher d_{33} than those with higher E_y . However, elastomers are non-electrets in most cases, partially because of their low glass transition temperature (T_g) which is well below room temperature. A low T_g can cause the relaxation of the dipole alignment of an electret after the charging. The introduction of voids into a polymer film with intrinsic high Young's modulus can be one strategy to reduce its overall E_y and endow it with the elastic-like behavior, which is appealing for both sensor and actuator applications [10, 11].

Patterns of electrostatic charges have been used in conventional xerography and can serve as templates to induce self-assembly and patterning of DNA, proteins and nanoparticles [12]. Moreover, micropatternable electrets can enable some specific applications in MEMS such as electrostatic motors, non-contact electrostatic micro-bearings and micro power generators [13, 14].

This paper proposes a material, suitable for electret formation, which can be viewed as a specially constructed polydimethylsiloxane (PDMS)/carbon-nanotubes (CNTs) composite. PDMS is an elastic, low cost, easily processible and bio-compatible insulator with a low Young modulus of 1–5 MPa and a high dielectric strength of 20 kV mm⁻¹. Carbon nanotubes exhibit excellent electrical properties with a charge density of 0.24 mC m⁻² for an individual tube [15] and can be micropatterned at room temperature [16]. The material proposed herein, the micropatterned PDMS/CNT composite, combines these two non-electret materials into a structure that can trap/store charges, allowing its potential utilization as a micropatternable squeezable/elastic electret. The proposed micropatterned PDMS/CNT composite was fabricated through a combination of electrophoretic deposition (EPD) and a transfer micromolding process. The EPD process cannot only pattern the CNTs, but also preserve the good rheological properties of unfilled PDMS and efficiently utilize the CNTs. Corona charging was exploited to implant charges into the composite and the electret-like and power generation of the charged elastic material were investigated.

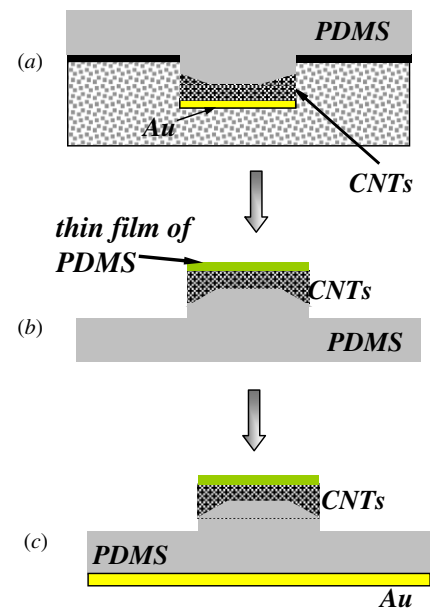


Figure 1. Scheme of the fabrication process for elastic Au/PDMS/CNT composite: (a) molding of micropatterned CNTs, (b) transfer micromolding of the CNT micropattern and (c) deposition of the gold backside electrode.

2. Development of the micropatterned elastic PDMS/CNT composite

2.1. Fabrication of the PDMS/CNT composite

Figure 1 depicts the fabrication process of the proposed electret material. Room temperature micropatterning of CNTs was achieved by EPD. Multi-wall CNTs (Nanostructured & Amorphous Materials, Inc., 95+%) were acidified in a mixture of concentrated sulfuric acid and nitric acid (3:1 volume ratio) to facilitate the EPD process. Carboxyl groups were thereby introduced onto the CNT, which improved the water dispersibility of the CNTs. Silicon substrates containing desired microstructures and a patterned gold seed layer were fabricated as the templates for EPD using standard microfabrication techniques. The microstructure-bearing substrates (anode) and a copper counter electrode (cathode) were immersed in a CNT aqueous dispersion (0.1 mg ml⁻¹) and electrically energized with an electric field of 20 V cm⁻¹. Under the electric field, the negatively charged CNTs migrate

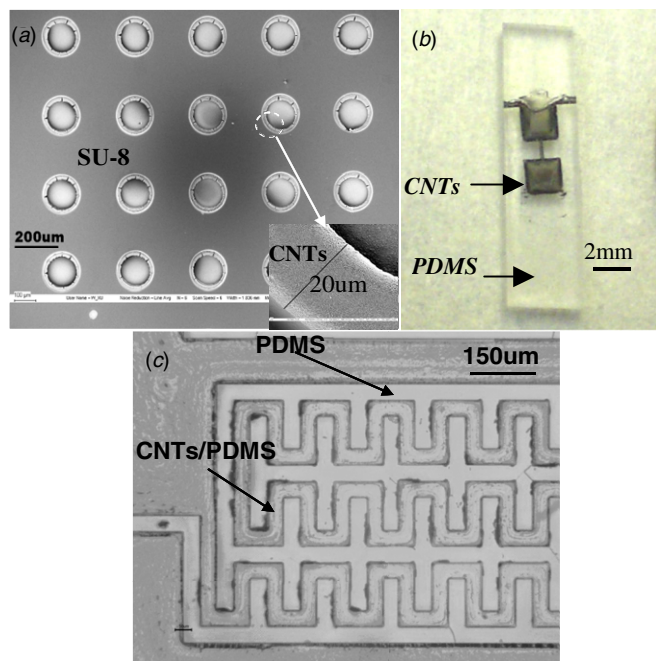


Figure 2. (a) SEM image of the CNT microwell array on SU8-bearing silicon template, (b) digital image of a CNT pattern on PDMS, (c) optical image of CNT micro-springs on PDMS.

toward the silicon template and precipitate on the regions bearing the gold patterns. The deposited mass, and therefore the thickness of the CNT layer, can be determined by the experiment duration for a given microstructure/dispersion deposition.

The fabricated micropatterns of the CNTs were then transferred into a PDMS matrix by pouring liquid PDMS precursor (Sylgard 184, Dow Corning) into the CNT micropatterns, curing it at 120 °C for 40 min, followed

by demolding the PDMS (figure 1(a)). Upon demolding, the CNT layer is transferred to the elastomeric PDMS film (figure 1(b)). Further details of the experiments and discussion of micropatterning of CNTs by EPD, as well as transfer micromolding with PDMS, have been previously reported [16]. A gold layer was then evaporated onto the non-CNT-bearing side of the PDMS sheet, serving as the backside electrode for the electret where the compensation charge may reside (figure 1(c)).

As presented in the following sections, scanning electron microscopy (SEM) (Zeiss, Ultra60) was exploited to observe the morphology of the CNT micropatterns and PDMS/CNTs composite structure, and energy-dispersive x-ray spectroscopy (EDS) was utilized to characterize the elemental composition of the topmost surface of the PDMS/CNT composite.

2.2. Micropatternability of CNTs through EPD

Different types of 2D/3D micropatterns of CNTs such as circular microwell arrays (figure 2(a)), micro-beams (figure 2(b)) and micro-springs (figure 2(c)) on either silicon/SU-8 templates or the elastic PDMS matrix can be achieved by the presented room temperature EPD and transfer micromolding process. EPD allows good control over the deposited CNT layer thickness, ranging from nanometers to tens of micrometers within 4 min [16].

2.3. Morphology of the patterned PDMS/CNT composite

Figure 3(a) is the SEM image of the top view of the CNT pattern on the PDMS matrix shown in figure 2(b). Figure 3(c) is the schematic view of the structure in figure 3(a). The SEM observation indicated that the CNTs were embedded underneath an ultra-thin film (figure 3(a)). Further element spectrum study by EDS at a low voltage (<4 kV) was performed to probe the uppermost layer (figure 3(b)). The

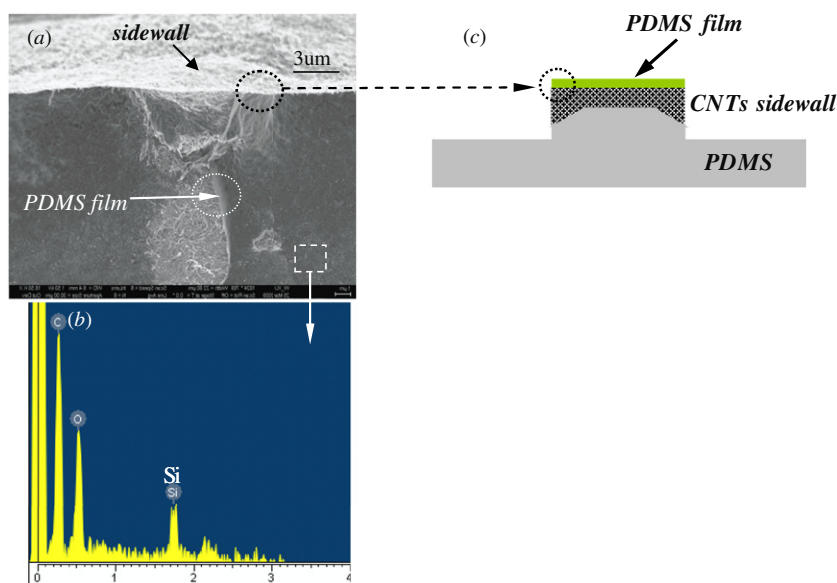


Figure 3. (a) SEM image of the top surface layer of the PDMS/CNT pattern in figure 2(b), (b) EDS spectrum of the top surface of the PDMS/CNT pattern and (c) schematic view of the structure in (a).

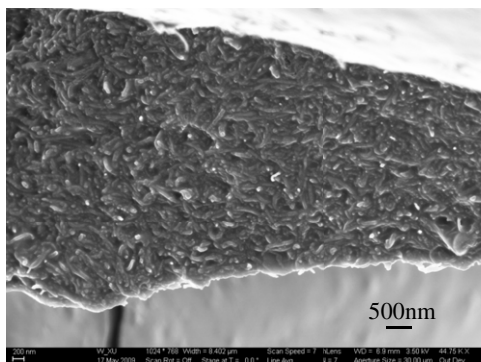


Figure 4. SEM image of the top view of the inner CNT layer.

elemental weight percentages of carbon, oxygen and silicon of the composite are consistent with those of unfilled PDMS (table 2). This thin PDMS film (~10 nm) was formed *in situ* during the micromolding process performed on the CNT patterns. During the PDMS molding process, the pre-polymer of PDMS flowed from the top surface of the porous CNT layer and gradually penetrated the network with the aid of vacuum degassing and capillary force. CNTs formed a random network at the interface with the bottom Au layer, instead of a dense monolayer that covers the whole interface. The contact area of each CNT with the bottom Au surface is small because of its cylindrical shape. So the prepolymer could fill the gaps and reach the bottom Au electrode, forming a quasi-continuous layer/film. The thin film may serve as an isolation layer between the CNTs and the external environment.

The SEM image of the CNTs layer in figure 4 showed that the CNTs were *in situ* coated with PDMS, forming a dense matrix that interpenetrated the CNT network. With the aid

Table 2. Elemental weight percentage.

Spectrum	C (weight%)	O (weight%)	Si (weight%)	Total (weight%)
PDMS/CNT composite	33.91	32.70	33.39	100
Unfilled PDMS	31.48	30.04	38.48	100

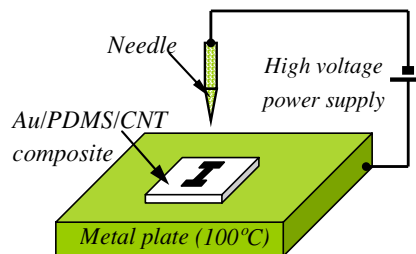


Figure 5. Schematic of the corona charging apparatus.

of vacuum degassing, the PDMS prepolymers penetrated and filled the voids in the CNT network during the micromolding process. As a result, a patterned CNT layer was sandwiched between an ultra-thin surface film (~10 nm) of PDMS and a bulk PDMS layer.

3. Investigation of the electret-like behavior of the composite

3.1. Corona charging

Negative charges were implanted into the sample films with a point-to-plane corona discharge method (figure 5). The sample was placed on a grounded metal plate with the CNT-bearing side facing upward under a stainless steel needle electrode.

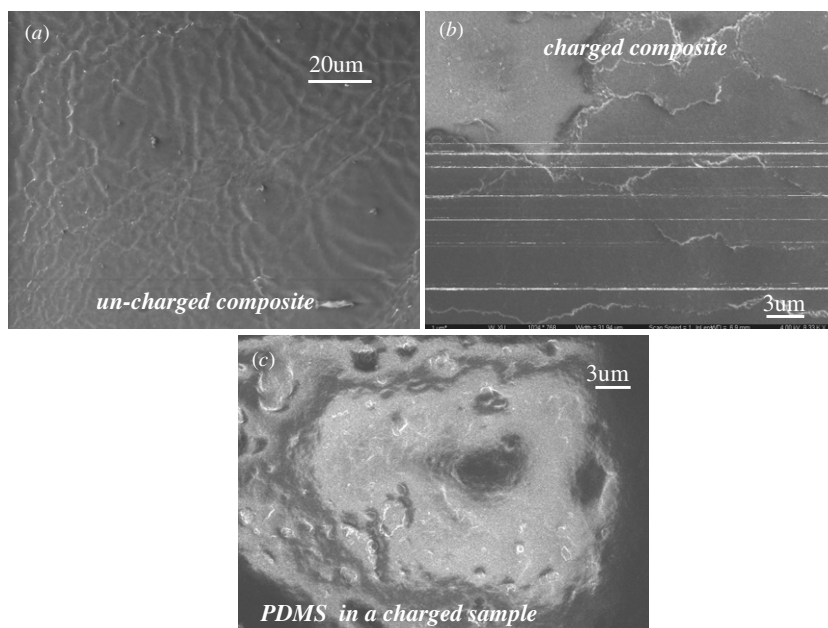


Figure 6. SEM image of (a) uncharged PDMS/CNT composite, (b) charged PDMS/CNT composite and (c) region with pure PDMS in a charged sample.

To maintain consistency across all materials investigated, the charging apparatus was placed inside an oven and heated to 100 °C. The distance between the tip of needle and the grounded plate was maintained at 15 mm. A constant voltage of -10 kV was then applied to the needle electrode for an hour. Afterward, the sample was first allowed to cool down to room temperature before the voltage was turned off. The decay of the surface charge density of the sample was then investigated by a surface potential voltmeter (surface dc voltmeter model SVM2, AlphaLab. Inc.).

SEM imaging of the composite was performed both before and immediately after the corona charging. Compared with the uncharged PDMS/CNT composite (figure 6(a)), the SEM image of the charged composite showed image distortion and interference (figure 6(b)). This likely represents the interaction of the charges in the electret after charging with the SEM electrons, demonstrating successful charging. Further imaging on the region composed of the pure PDMS in a charged sample showed no such phenomenon (figure 6(c)), which may indicate much more rapid decay/relaxation of the charge/dipole alignment in the pure PDMS than that in the PDMS/CNT composite region.

3.2. Study of charge storage stability

To understand the charge storage mechanism of this non-traditional material composed of two non-traditional electrets, three different reference samples were investigated for comparison: PDMS with no CNTs, PDMS with a cast CNT layer as opposed to an embedded/molded layer (PDMS/cast-CNTs), and a gold layer sandwiched between a thin film (~10 nm) of PDMS and a bulk PDMS layer (PDMS/Au/PDMS). These were fabricated and charged under the same corona charging conditions as the original PDMS/CNTs. In addition, in order to compare the performance of the composite with the traditional electrets, a 300 μm thick Teflon film was charged with the same corona charging apparatus. The surface charge stability of all five samples was then characterized as a function of time with a surface potential voltmeter.

As listed in table 3, the PDMS/CNT composite and the Teflon exhibited much higher initial surface charge density than those of the other three reference samples. The surface charge density (Q/A) of the PDMS/CNTs composite underwent a sharp drop to 26% of its initial value within the first 30 min, and then exhibited a relatively stable plateau, at around 5% of the initial value, for the ensuing measurement duration of 280 h (figure 7). Relative to the PDMS/CNTs, the three reference samples all exhibited much faster decay of the surface charge density, no stable plateau and complete charge exhaustion in less than 5 h (bottom graph in figure 7).

The results may indicate that (1) the charges injected into the pure PDMS are unstable and tend to dissipate within a short period of time, which is consistent with the results reported by Nguyen *et al* [19]; (2) pure CNTs without being encapsulated by a PDMS dielectric layer could not store charges for an extended time either; and (3) the charge retention capacity of the CNTs embedded in the PDMS may not be due only to

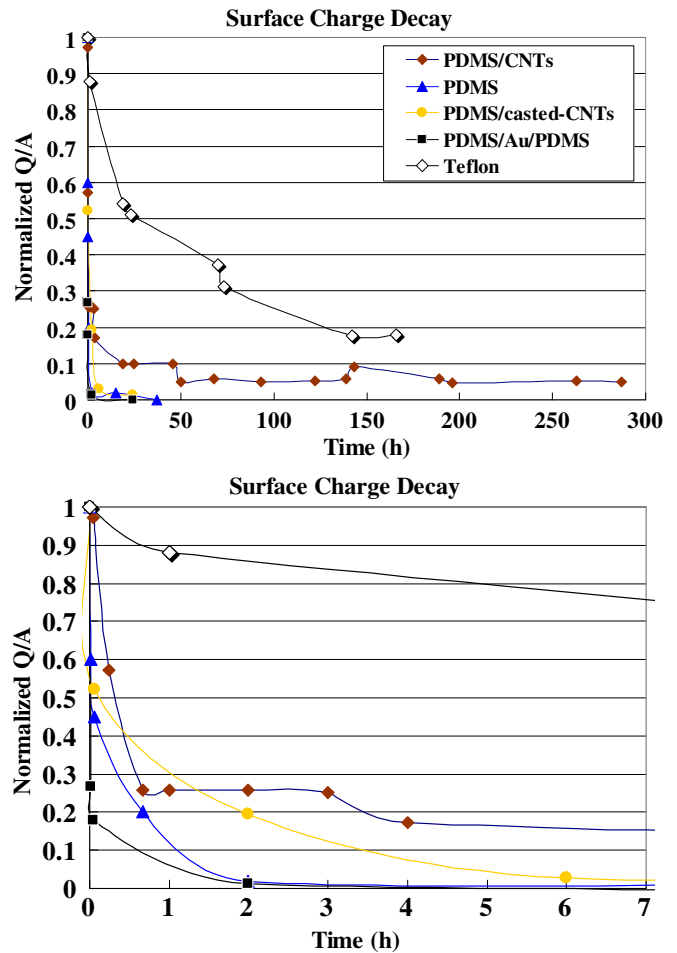


Figure 7. Top: decay curves of the surface charge density (Q/A). Bottom: enlarged decay curve of the first 7 h. The surface charge density in all cases has been normalized to its value at $t = 0$.

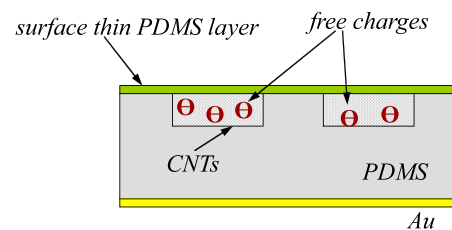


Figure 8. Proposed charge storage mechanism of the elastic PDMS/CNT composite.

the conductivity of the CNT, since the sample with the gold layer as the charge trapping layer did not exhibit stable charge storage.

Since there is a significant difference in charge storage behavior between PDMS/CNT composite materials and pure PDMS, it is reasonable to conclude that charges can penetrate the topmost ultra-thin PDMS film and be trapped by the CNTs during the corona charging (figure 8). The thin PDMS dielectric layer may act as an energy barrier to prevent the injected charges in the CNTs from escaping to the outer environment. As a result, the PDMS/CNT composite shows higher long-term surface charge stability than either pure PDMS or pure CNTs. In this case, the patterning

Table 3. Initial surface charge density.

Sample	PDMS/CNTs	PDMS	PDMS/casted-CNTs	PDMS/Au/PDMS	Teflon
Initial surface charge density (C cm ⁻²)	4×10^{-9}	3×10^{-10}	3×10^{-11}	6×10^{-11}	1×10^{-9}

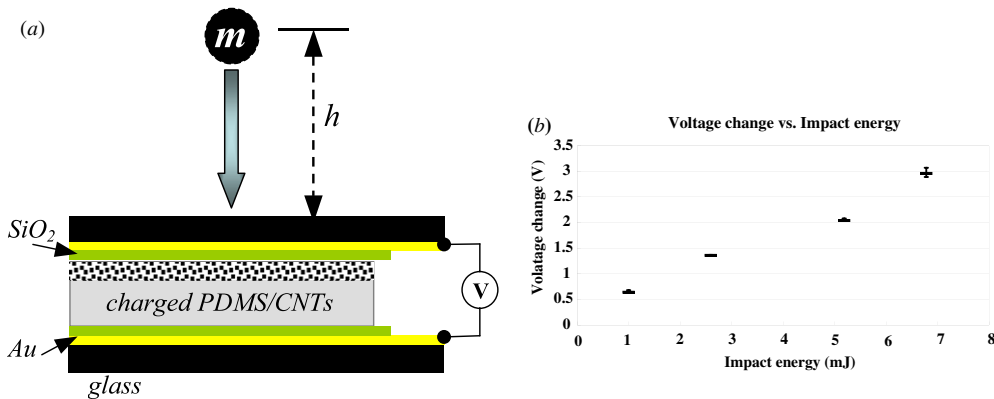


Figure 9. (a) Scheme of the ball drop experiment and (b) voltage change as a function of impact energy ($E = mgh$).

of electrostatic charges can also be achieved through the patterning of the CNTs. However, compared with some other non-elastic polymer electrets, such as Teflon, charged/stored under the same conditions, the elastic PDMS/CNT composite material still suffers faster charge decay (figure 7). This may be partially attributed to the high volatile gas/vapor permeability and the relatively low volume resistivity of PDMS ($\sim 10^{14} \Omega \text{ cm}$), in contrast to the Teflon, which has a higher resistivity of $10^{18} \Omega \text{ cm}$ and much higher hydrophobicity. The charge storage stability of the proposed micropatternable elastic material could potentially be improved by utilizing other elastomers with a lower electrical conductivity and lower vapor permeability as the matrix.

4. Evaluation of the power generation of the charged elastic composite

To test the potential power generation of the charged composite, a ball drop experiment was performed (figure 9(a)). In order to electrically connect the CNT/PDMS sensor structure, a 500 nm thick gold electrode was first deposited on a glass slide with an E-beam evaporator, followed by the deposition of a 1 μm thick silicon dioxide layer on top of it through a plasma-enhanced chemical vapor deposition (PEVCD) process. A metal wire was then fixed to the one end of the gold electrode using silver epoxy. A corona-charged PDMS/CNT composite was sandwiched between two glass substrates bearing the two-layer coatings. The assembled structure was further connected to an oscilloscope (Tektronix TDS 2014, 1 M Ω input impedance) through the two metal wires on the top and bottom glass substrates. A steel ball with a mass (m) of 4.07 g and a diameter of 10 mm was centered above the top glass slide and subjected a free fall from various heights (h). The output voltage of the sample was then recorded by the oscilloscope.

From the curves in figures 9(b) and 10, a monotonic increase of voltage change across the charged composite

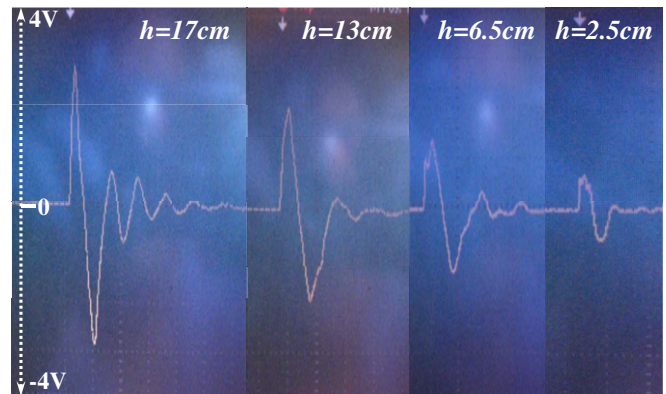


Figure 10. Curve of the voltage change of the sample as a function of time in response to different heights of the ball drop.

was observed with the increased impact energy ($E = mgh$), which may lead to potential applications in vibration-based energy harvesters. More detailed studies are underway to fully characterize its performance in power generation.

5. Summary

An elastic PDMS/CNT composite suitable for elastic electrets and its charged electrical behavior have been discussed in this paper. The proposed PDMS/CNT composite combines the micropatternability of CNTs and the elasticity of PDMS. Charge storage stability has been measured in excess of 280 h. The power generation behavior of the corona-charged composite was also demonstrated through a ball drop experiment. Elastic electrets have the potential for integration into devices or microsystems such as flexible power generators, MEMS electret microphones, loudspeakers, artificial muscles and robots, or piezoelectric sensor/actuators.

Acknowledgments

The authors would like to thank Richard Shafer for help on the characterization of the devices and Chao Song for assistance in the ball drop experiment.

References

- [1] Baeg K J, Noh Y Y, Ghim J, Lim B and Kim D Y 2008 Polarity effects of polymer gate electrets on non volatile organic field-effect transistor memory *Adv. Funct. Mater.* **18** 3678–85
- [2] Altafim R A P 2009 Template-based fluoroethylenepropylene piezoelectrets with tubular channels for transducer applications *J. Appl. Phys.* **106** 014106
- [3] Wu T Z, Suzuki Y and Kasagi N 2008 Electrostatic droplet manipulation using electret as a voltage source *Proc. IEEE Int. Conf. MEMS (Tucson)* pp 591–4
- [4] Naruse Y, Matsubara N, Mabuchi K and Suzuki S 2009 Electrostatic micro power generation from low-frequency vibration such as human motion *J. Micromech. Microeng.* **19** 094002
- [5] Amjadi H 1999 Charge storage in double layers of thermally grown silicon dioxide and APCVD silicon nitride *IEEE Trans. Dielectr. Electr. Insul.* **6** 852–5
- [6] Resnick P R and Buck W H 2002 *Fluoropolymers 2* (Berlin: Springer) pp 25–33
- [7] Sakane Y, Suzuki Y and Kasagi N 2008 The development of a high-performance perfluorinated polymer electret and its application to micro power generation *J. Micromech. Microeng.* **18** 104011
- [8] Ogawa G, Sugiyama N, Kanda M and Okano K 2005 Perfluoro transparent resin ‘Cytop’—some physical properties and kinetic studies on radical polymerization reaction *Rep. Res. Lab. Asahi Glass Co., Ltd* **55** 47–51
- [9] Lushcheikin G A 2006 New polymer-containing piezoelectric materials *Solid State Phys.* **48** 1023–5
- [10] See <http://www.azom.com/Details.asp?ArticleID=398>
- [11] Altafim R A C, Basso H C, Altafim R A P, Lima L, Aquino C V D and Neto L G 2006 Piezoelectrets from thermo-formed bubble structures of fluoropolymer-electret films *IEEE Trans. Dielectr. Electr. Insul.* **13** 979–85
- [12] Zhao D, Duan L, Xue M, Ni W and Cao T 2009 Patterning of electrostatic charge on electrets using hot microcontact printing *Angew. Chem., Int. Ed.* **48** 6699–703
- [13] Tsurumi Y and Suzuki Y 2008 Non-contact electrostatic micro-bearing using polymer electret *Proc. IEEE Int. Conf. MEMS 2008 (Tucson, AZ)* pp 511–4
- [14] Sakane Y, Suzhuki Y and Kasagi N 2008 The development of a high performance perfluorinated polymer electret and its application to micro power generation *J. Micromech. Microeng.* **18** 104011
- [15] Jespersen T S and Nygård J 2005 Charge trapping in carbon nanotube loops demonstrated by electrostatic force microscopy *Nano Lett.* **5** 1838–41
- [16] Xu W J and Allen M 2009 Fabrication of patterned carbon nanotube (CNT)/elastomer bilayer material and its utilization as flexible force sensors *Tech. Dig. Int. Solid-State Sensors, Actuators and Microsystems Conf. (Denver)* pp 2242–5
- [17] Lo H W and Tai Y C 2008 Parylene-based electret power generators *J. Micromech. Microeng.* **18** 104006
- [18] Amjadi H 1999 Charge storage in double layers of thermally grown silicon dioxide and APCVD silicon nitride *IEEE Trans. Dielectr. Electr. Insul.* **6** 852–7
- [19] Nguyen D H, Sylvestre A, Bechu S and Rowe S 2004 Estimation of surface degradation under immersion plasma by surface potential decay method *Electrical Insulation and Dielectric Phenomena, Annu. Rep. Conf. 2004 (Colorado)* pp 631–4